De: Milan M Antonijevic <editor.ijes@esgpublisher.com>
Fecha: El mar, 20 de marzo de 2018 a la(s) 02:26
Asunto: RE: Paper - 1207125 - Leon
Para: Daimir LL <luis_lopez@uaeh.edu.mx>

Dear dr Leon, I would like to inform you that your revised paper (1207125) <u>has been accepted for publication in our journal.</u>

Thank you for your contribution.

Best regards

M. Antonijevic

Editor

International Journal of Electrochemical Science

www.electrochemsci.org

From: Daimir LL [mailto:luis_lopez@uaeh.edu.mx]
Sent: 20 March 2018 07:40
To: Milan M Antonijevic
Cc: Gonzalo Gonzalez
Subject: Re: Paper - 1207125 - Leon

Dear Prof. Antonijevic:

The revised paper has been edited according with the last observations.

Regards

Dr. Luis Daimir López León

Electrochemical behavior of carbon steel under a continuous kerosene flow in two different kinds of sections.

I. E. Castaneda-Robles[1], L. D. López-León[1], V. M. Moreno-Landeros[2], M. A. Baltazar-Zamora[3], F. J. Olguín-Coca[1], L. G. Lizárraga-Mendiola[1]*

[1] Cuerpo Académico de Ingeniería Civil Sustentable y Tecnología de Materiales, Universidad Autónoma del Estado de Hidalgo, Carr. Pachuca-Tulancingo km 4.5 Col. Carboneras, Mineral de la Reforma 42184, México.
[2] Facultad de Ingeniería Civil, Universidad Autónoma de Coahuila, Unidad Torreón, Carretera Torreón- Matamoros, km 7.5 Ciudad Universitaria, Torreón, Coahuila, C.P. 27276, México.
[3] Facultad de Ingeniería Civil - Xalapa, Universidad Veracruzana, Circ. G. Aguirre Beltrán S/N, Lomas del Estadio, Xalapa, Veracruz. C.P. 91000, México.
[*]E-mail: luis_lopez@uaeh.edu.mx

This work studies the electrochemical behavior of carbon steel under a continuous kerosene flow in two different kinds of sections: a linear section and a 90-degree horizontal elbow section. To apply the electrochemical techniques, two experimental arrangements were designed, one with the electrochemical cell in a linear section and the other with the cell in an elbow. The electrochemical techniques used were polarization curves and electrochemical impedance spectroscopy (EIS). The polarization curves obtained indicated that the values of Icorr, as well as the density of current, increased significantly for the cell placed in the elbow section. Corrosion velocity values show that there is a difference between the experimental arrangements. The EIS technique shows that for the arrangement with the cell in an elbow, the resistance of steel to corrosion is lower than for the arrangement with the cell in a linear section. The presence of kerosene in steel modifies the corrosion process and avoids the formation and growth of a passive layer, in which the corrosive agents adsorption increases. Analysis with XPS showed that the system with the cell in a 90-degree horizontal elbow section increases crystal deposits of chloride ions on the metal surface.

1. INTRODUCTION

Corrosion is an unavoidable process; however, techniques have been developed to delay it, therefore extending the useful life of materials. Finding these techniques has required technical and experimental work to reach these critical advances in the field of corrosion. Moreover, the petroleum industry is one of the most important industrial complexes in the world. Carbon steel is a highly reliable metallic alloy used in the petroleum industry because of its high resistance and low cost. Hydrocarbons generated from the petroleum industry contain impurities of distinct elements, and these impurities have an important role in the area of corrosion of metallic materials such as carbon steel [1-6]. The transport of dangerous and inflammable fluids, such as petroleum, natural gas and distinct hydrocarbons, through pipelines has been found to be economically viable, compared to other ways of transport, such as by rail or road [7]. The integrity and stability of pipelines becomes important when discussing economic impact and safety; therefore, the study of corrosion resistance of metallic materials used in hydrocarbon transport has driven the study of different parameters to reduce the phenomenon of corrosion [8,9]. On the other hand, electrochemical properties of carbon steel are part of several studies, due to the varied applications of this material in the petroleum industry, such as in boilers, heat exchange systems and as construction material of petroleum refining equipment, storage tanks and hydrocarbon transport pipelines [10,13]. In this industry, interior corrosion in pipelines is primarily caused by the presence of dissolved salts rich aqueous phase (brine). The corrosiveness of salts transported along with hydrocarbons, is increased by the presence of gases, such as hydrogen sulfide (H_2S) and carbon dioxide (CO_2), flowrate, temperature, acidity and the presence of sediments, among others. These factors contribute to different corrosion scenarios that can coexist on different sections of the same pipeline [14-16]. The method NACE 1D196 is one of the most used in the petroleum industry to evaluate metallic materials and materials with some inhibitors on the surface. This method states that the interaction of chlorides with metal (where the adsorption processes govern the corrosion mechanism) could be modified by the presence of other phases, such as hydrocarbons, as it occurs in the petroleum industry. In addition, corrosion process can be modified by the presence of hydrocarbon causing damages or an increase in the corrosion speeds, so it is important to know and reproduce real environments where corrosive agents are involved, system flow and hydrocarbon [18,19]. In this work, the corrosion of an AISI 1018 pipeline steel in oil-water emulsions was investigated using a pipe flow system designed and constructed by the authors. In order to find the effect of immiscible mixtures on the corrosion of carbon steel, the process was studied for an experimental arrangement with an electrochemical cell in a linear section and an experimental arrangement with an electrochemical cell in a 90-degree horizontal elbow section, were studied [17] in a solution similar to NACE 1D196 in the absence and presence of kerosene. Electrochemical measurements, including electrochemical impedance spectroscopy (EIS) and potentiodynamic polarization curves, were conducted to determine the corrosion mechanism and rate under the selected experimental conditions. Parametric effects, such as flow velocity, electrochemical cell placement in the system, temperature and the content of oil in the fluid, on steel corrosion were determined.
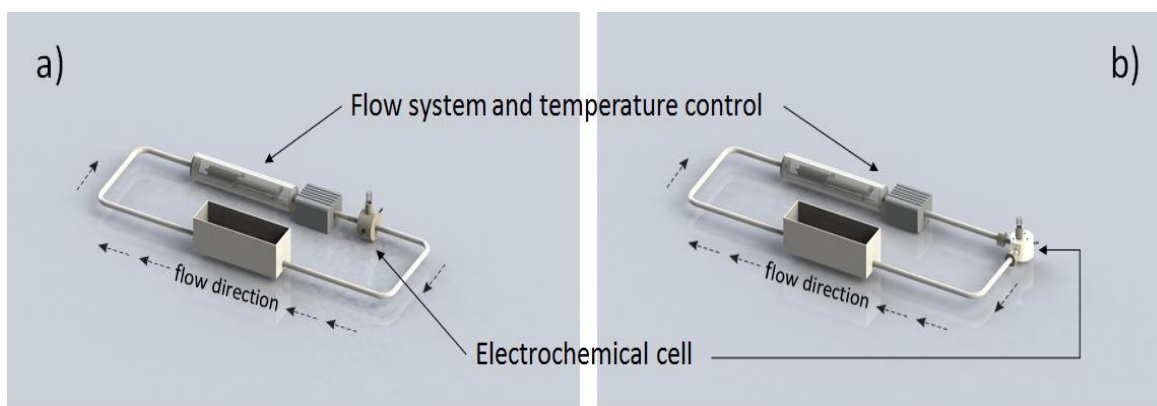
2. EXPERIMENTAL

2.1. Experimental Setup

Two experimental arrangements were used to study corrosion in different sections: in the first section the electrochemical cell was located in a linear section and in the second section the electrochemical cell was located in a 90-degree horizontal elbow section (Figure 1). For the electrochemical techniques the electrochemical cell configuration was a saturated calomel electrode as reference electrode and a graphite bar as counter electrode.

As working electrodes, bars of AISI 1018 carbon steel (C 0.18%; Mn 0.70%; Si 0.20%; P 0.05%; S 0.07%) were used and connected to a polymeric support (Figure 2). For each experiment, the surface of the working electrode was grinded and polished with SiC paper (grade 280).

The corrosive environment established by the NACE 1D196 [20] was used to evaluate the different sections [21], with the following composition: 85.07 g calcium chloride dihydrate, 39.16 g magnesium chloride sixhydrate, 2.025 g sodium chloride, 19 L distilled, saturated with CO_2 (oxygen content less than 10ppm) in the absence and presence of kerosene in a ratio of 8:2.

The solution was prepared with deionized water and deaerated with high purity nitrogen for 30 min. The following reagents were used (A. R. grade): 99% purity NaCl (Baker); 100% purity hexahydrated $MgCl_2$ (Baker), 99% purity dehydrated $CaCl_2$ (Baker) and kerosene from Baker. Once the brine was prepared, it was purged with CO_2 (30 minutes per liter of brine) with a controlled pressure of 0.70 kg/cm^2.

Figure 1. Experimental arrangement a) Electrochemical cell placed in a linear section b) Electrochemical cell placed in a 90-degree horizontal elbow section.
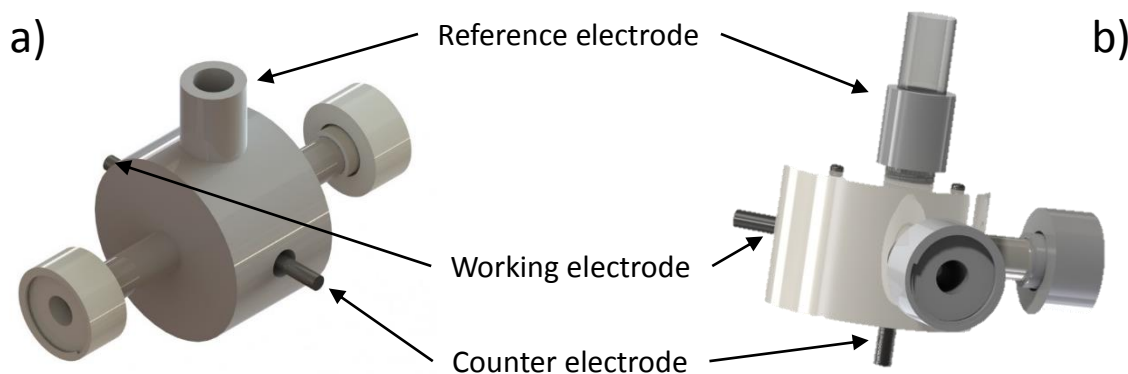
Figure 2. Electrochemical cell a) for a linear section b) for an elbow section.

The experiments were performed at a temperature of $50 \pm 1 \,^\circ$ C, after a corrosion potential stabilization (15 minutes immersion of the working electrode) and with a flow rate of the corrosive environment of 7.5 liters per minute. The potentiodynamic polarization curves were registered at a scan rate of 0.1 mV/s in a potential range between $-$ 300 to 300 mV (vs. o.c.p.) and each curve was obtained from a freshly abraded steel surface. The electrochemical impedance spectroscopy (EIS) measurements were carried out with an amplitude of 10 mV (vs. o.c.p.) and in the frequency range of 10 mHz to 10 kHz. A Potentiostat-Galvanostat Autolab Mod PGSTAT30 with Frequency Response Analyzer (FRA) was used and managed through the software of the same company.

For the XPS study, samples were analyzed on the Thermo Scientific 260Xii using XPS, spectroscopic imaging and depth profiling. The samples were coupled on conventional supports and fixed with conductive tape. The XR6 monochromated X-ray source was used for XPS analysis, to help obtain a fixed point, and was selectable by the analyst in the range of 250-900 μm. A 900 μm X-ray spot was used to give high sensitivity, to allow rapid data processing and to ensure good coverage in XPS imaging; the 400 μm spot was used for depth profiling. All data processing was performed within the Advantage data system.

3. RESULTS AND DISCUSSION

3.1 Potentiodynamics Polarization Curves (without kerosene)

Figure 3 shows the potentiodynamic polarization curves obtained from the electrochemical cells in both sections in absence of kerosene. From the Figure 3 it can be appreciated that the corrosion density values are higher for the experimental arrangement with the electrochemical cell in the elbow section. Potentiodynamic polarization curves in Figure 3 exhibited an active behavior, corresponding

to a charge transfer process. It can also be seen that corrosion potentials show difference depending on the location of the electrochemical cell, where the linear section presents nobler potential values. The corrosion potential in the section is −690±50 mV vs Hg/HgCl(s)/KCl(sat) (SCE), indicating that the initial conditions of the surface are similar.
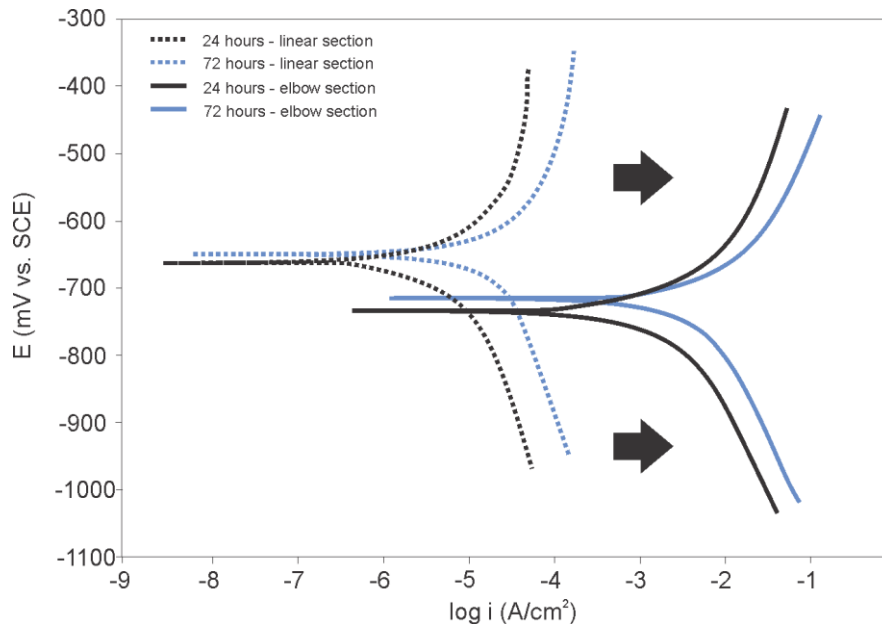
Figure 3. Polarization curves obtained for carbon steel system AISI 1018 immersed in solution type NACE 1D196 to evaluate the cell placed in a linear section and the cell placed in an elbow section behaviors in the absence of the kerosene.

3.2 Potentiodynamic Polarization Curves (with kerosene)

Figure 4 shows the potentiodynamic polarization curves for the systems considering immersion time and presence of kerosene. It can be seen that obtained currents are higher than the ones obtained without kerosene, presenting higher current values in the elbow section. The corrosion potential in the system is −760 ± 30 mV vs Hg/HgCl(s)/KCl(sat) (SCE).
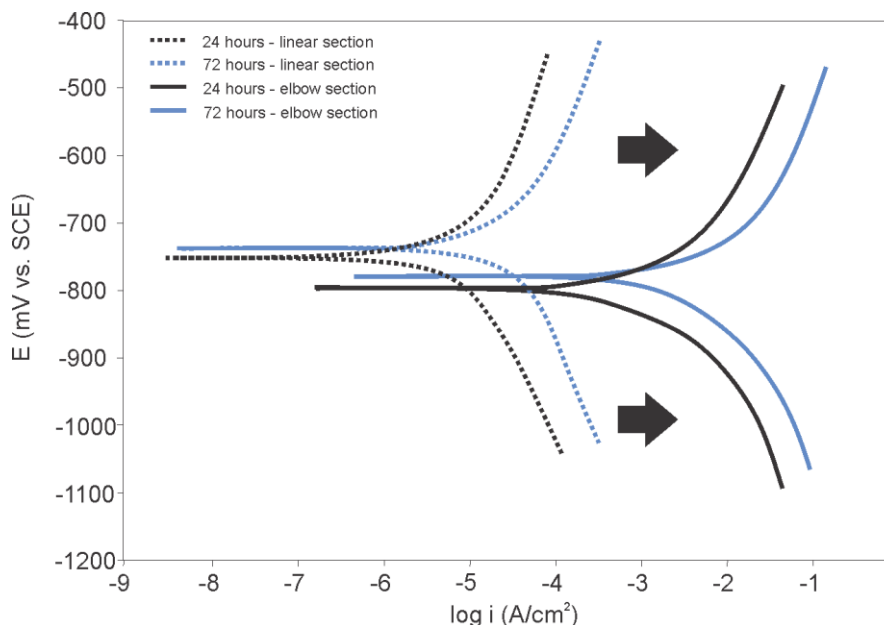
Figure 4. Polarization curves obtained for the carbon steel section in solution type NACE 1D196 to evaluate the linear section and the elbow section behaviors in presence of the kerosene.

3.3 Corrosion parameters obtained from potentiodynamic polarization curves

Table 1 shows the corrosion parameters obtained for the systems in presence and in absence of kerosene.Kerosene presence favors the diffusive processes with the anodic and cathodic slopes showing a different behavior with increasing slopes, with a higher effect in the cathodic branch. Moreover, the anodic slopes show some differences for the elbow section. Nevertheless, the values of the anodic slope suggest a large activity on the surface and control in the change of transference. Analysis of the Icorr values shows that for the elbow section, the Icorr increases significantly compared to the linear section.

The specific adsorption of chloride ions Cl$^-$ in the corrosive environment appears to be modified by the electrochemical cell location in the section, favoring its arrival to the metal surface in the elbow section, which results in an increase of the cathodic current. However, there are also diffusive processes that become more important with the presence of kerosene, which are manifested in an increase in the cathodic slope.

Table 1. Corrosion parameters obtained for the sections.

Corrosion parameters of carbon steel sections			Ecorr (V)	ba (V/dec)	bc (V/dec)	Icorr (A/cm^2)
Without kerosene	Linear section	24 hrs.	-0.66	0.0750	-0.289	5.32E-05
		72 hrs.	-0.64	0.0792	-0.249	4.73E-04
	Elbow section	24 hrs.	-0.73	0.0783	-0.269	2.52E-03
		72 hrs.	-0.71	0.0743	-0.255	1.97E-03
With kerosene	Linear section	24 hrs.	-0.75	0.0862	-0.284	4.93E-05
		72 hrs.	-0.73	0.0856	-0.269	4.33E-04
	Elbow section	24 hrs.	-0.79	0.0877	-0.283	2.12E-03
		72 hrs.	-0.78	0.0895	-0.298	1.47E-03

3.4 Impedance behavior of the section without kerosene

Figure 5 shows Nyquist diagrams with the results of the Electrochemical Impedance Spectroscopy technique for the sections in the presence of the corrosive solution without kerosene, considering the immersion time of the electrode. The spectrum shows similar behaviors containing two visible segments; the first is a capacitive semicircle, which can be attributed to charge transference, located at high frequencies and the second is a linear segment corresponding to a diffusive process located at low frequencies. The values of real and imaginary impedance diminish as the immersion time increases for both experimental arrangements, lower impedance values were presented in the elbow section, which is related with high corrosion velocities.
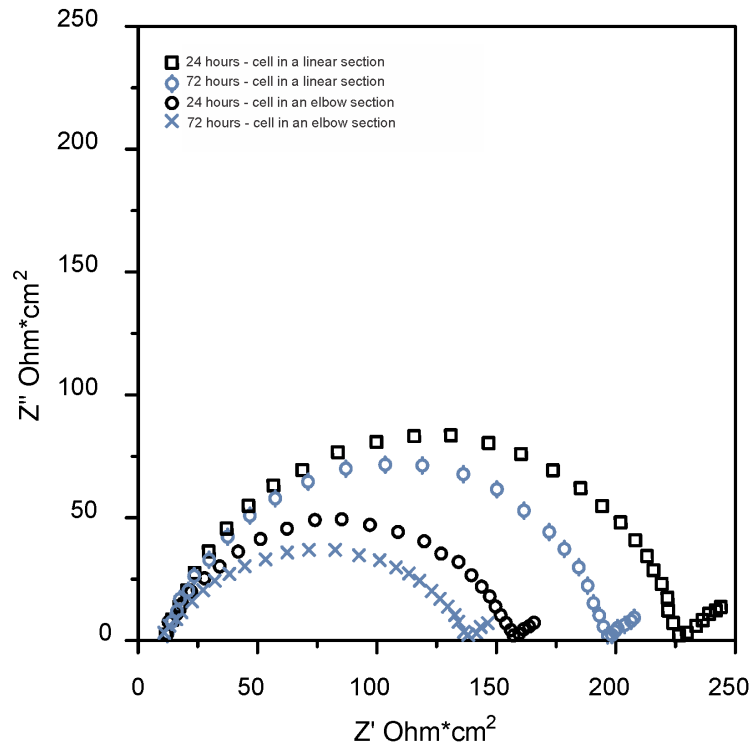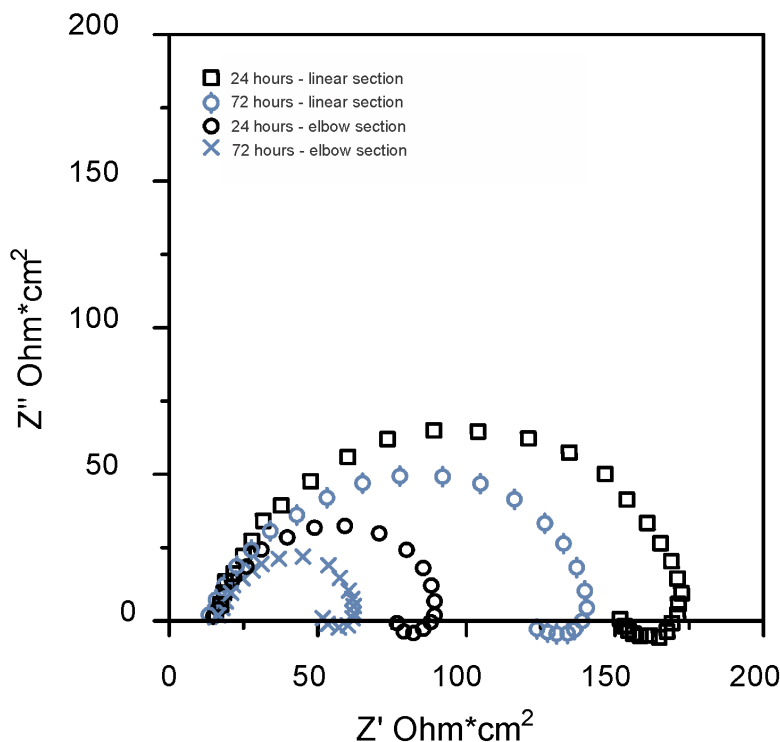
Figure 5. Nyquist diagram for the sections of carbon steel in a solution of NACE 1D196 on a linear section and in an elbow section behaviors without kerosene.

3.5 Impedance behavior of the sections with kerosene

Figure 6 shows Nyquist diagrams for AISI 1018 steel immersed in a corrosive medium (NACE 1D196 solution) in presence of kerosene. The obtained spectrum presents a semicircle segment located at high frequencies, corresponding to a charge transfer process, and a loop segment located at low frequencies, which corresponds to a chemical species adsorption process. This fact can be related to the competitive adsorptive process that takes place on the metal surface [22,23]. Figure 6 also presents the Rs values, which are very similar for the sections studied. The elbow section showed lower values of Rp.

The presence of the kerosene in both corrosion sections promoted the adsorption of corrosive species on the metal surface, causing more damage in the elbow section.

Figure 6. Nyquist diagram for the sections of carbon steel in a solution of NACE 1D196 with the cell placed in a linear section and the cell placed in an elbow section behaviors in presence of kerosene.

3.6 Corrosion parameters obtained from the Electrochemical Impedance Spectroscopy technique

**Table 2.** Corrosion parameters obtained from the Electrochemical Impedance Spectroscopy technique.

Corrosion parameters of carbon steel sections			Ecorr (V)	Rs/Ω	Rp/Ω
Without kerosene	Linear section	24 hrs.	-0.66	12.5	217.6
		72 hrs.	-0.63	14.6	175.2
	Elbow section	24 hrs.	-0.74	15.4	145.1
		72 hrs.	-0.71	13.7	122.4
With kerosene	Linear section	24 hrs.	-0.75	16.4	154.3
		72 hrs.	-0.72	13.3	116.8
	Elbow section	24 hrs.	-0.79	15.9	70.6
		72 hrs.	-0.77	17.0	38.2

Ecorr values are higher when there is kerosene in the system, as shown in Table 2. This indicates that adding kerosene causes a more aggressive environment for both experimental arrangements, presenting even more corrosive damage in the elbow section. It can be observed that Rp

values are lower for the elbow section. Higher Rp values correspond to the linear section without kerosene.systems with.

According to the results obtained from the EIS, two processes take place at low frequencies, which modify the working electrode polarization resistance: diffusion and adsorption. A diffusion process occurs in absence of kerosene for both experimental arrangements and an adsorption process takes place in both experimental arrangements when kerosene is introduced in the system, Rp values decreased due to the adsorption process. In the presence of kerosene it can be stated that the general mechanism of the anodic process for the sections is similar to the proposed by Li et al.,[25], where metal dissolution occurs primarily by adsorption.

3.7 X-ray Photoelectron Spectroscopy
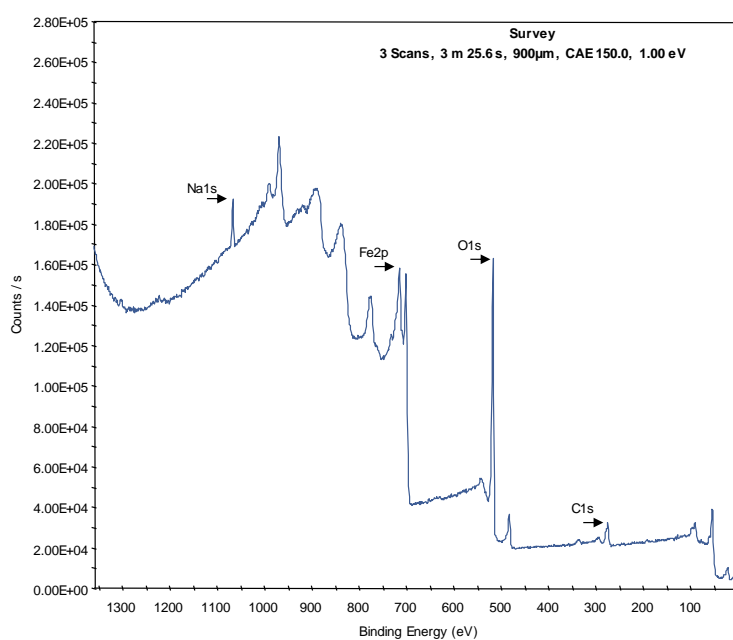
Figure 7. XPS Survey Spectrum of the working electrode for the linear section in presence of kerosene.

Spectrum in Figure 7 shows that the working electrode from the linear section and in presence of kerosene has C, O, Na and Fe and traces of elements at non-significant concentration. Spectrum in Figure 8 shows that the working electrode from the elbow section and in presence of kerosene has C, O, Na, Fe and Cl.
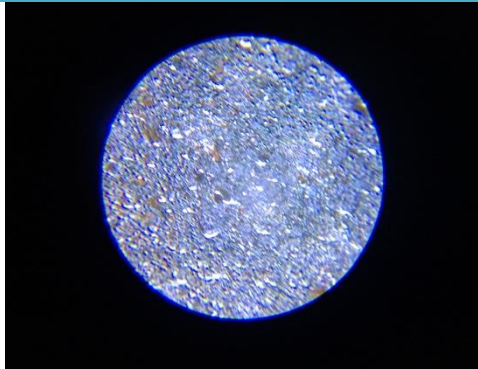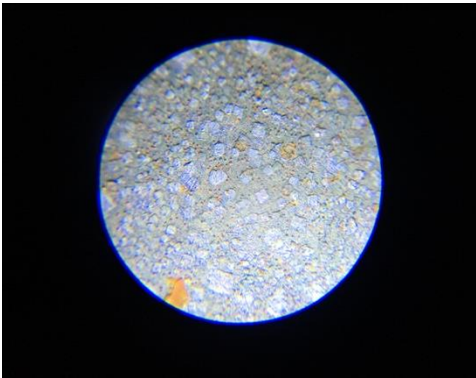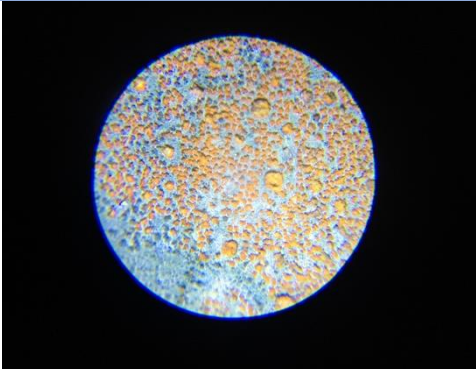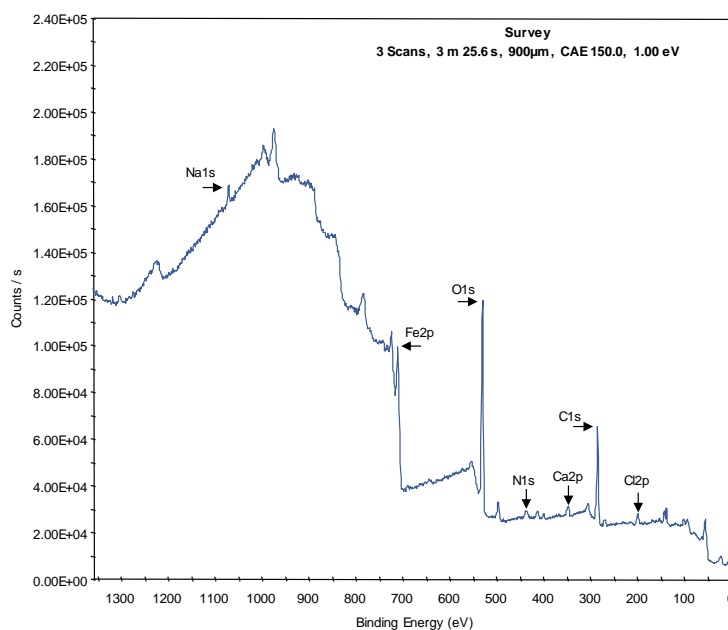
Figure 8. XPS Survey Spectrum of the working electrode of the elbow section in presence of kerosene.

The results show that the intensity of iron increases significantly, the intensity of sodium across the analyzed profile is constant, the calcium has a slight increase in comparison to the previous spectrum and the chlorine increases in all intensities [26,27].

Micrographs from Table 3 corroborate the results obtained from EIS technique. It can be seen that corrosive damage on the working electrode surface is higher for the experimental arrangements with the electrochemical cell located in an elbow section. From EIS was noticed that in presence of kerosene the polarization resistance decreased, causing severe corrosive damage, which can be observed in micrographs. Micrograph corresponding to the working electrode from the elbow section and in presence of kerosene shows abundant corrosion products.

Table 3. Micrographs of AISI 1018 steel used as working electrode in the studied sections.

Corrosion parameters of carbon steel sections		Micrographics 60x
Without kerosene	Linear section	

	Elbow section	
With kerosene	Linear section	
	Elbow section	

4. CONCLUSIONS

Corrosion damage varies depending on the section where the electrochemical cell is located in the system. In addition to charge transfer process, there are two corrosion processes involved: diffusion for the sections in presence of kerosene and adsorption for the sections in absence of kerosene.

From the Nyquist diagrams obtained by EIS technique it can be seen that there are capacitive semi-circles at high frequencies for all cases. Sections in presence of kerosene show inductive arcs in the lower part of the semicircle at low frequencies, while sections in absence of kerosene present a diffusive linear segment at low frequencies. Inductive arcs can be attributed to the concentration augment of a chemical specie (chloride, Cl^-) which is adsorbed on the working electrode surface and that is involved in the surface dissolution process.

Adsorption process promotes the deposition of corrosive agents on the metal surface. Therefore corrosion velocity augments significantly due to the location of the electrochemical cell in the experimental arrangement, which can be explained by hydrodynamic parameters for the elbow section.

XPS results show the presence of chloride ions on the working electrode surface of the elbow section in presence of kerosene.

References

1. Q.L. Wu, Z.H. Zhang, X.M. Dong and J.Q. Yang, *Corros. Sci.,* 75 (2013) 400.
2. H. Hu and Y.F. Cheng, *J. Pet. Sci. Eng.,* 146 (2016) 134.
3. W. Li, B. Brown, D. Young, S. Nešic, *Corrosion,* 70 (2014) 294.
4. J. Thaker and J. Banerjee, *J. Pet. Sci. Eng.,* 145 (2016) 298.
5. O. Yevtushenko, R. Bäßler and A. Pfennig, *Mater. Corros.,* 63 (2012), 517.
6. V.F. Lvovich and M.F. Smiechowski, *Electrochim Acta,* 51 (2006), pp. 1487.
7. C.E. Restrepo, J.S. Simonoff, R. Zimmerman, *Int J Crit Infrastruct Prot,* 2 (2009) 38.
8. J.L. Alamilla, E. Sosa and C.A. Sanchez-Magana, *Mater. Des.,* 50 (2013) 766.
9. Y. Wang, G. Cheng and W. Wu, *Appl. Surf. Sci.,* 349 (2015) 746.
10. M. Gao, X. Pang and K. Gao, *Corros. Sci.,* 53 (2011) 557.
11. M.M. Osman and M.N. Shalaby, *Mater. Chem. Phys*. 77 (2003) 261.
12. P.C. Okafor, X. Liu and Y.G. Zheng, *Corros. Sci*. 51 (2009) 761.
13. B.H. Zhou and Z.Q. Zhai, *Eng. Fail. Anal.,* 18 (2011) 1333.
14. V. Garcia-Arriaga, J. Alvarez-Ramirez, M. Amaya and E. Sosa, *Corros. Sci*. 52 (2010) 2268.
15. P. Altoe, G. Pimenta, C.F. Moulin and O.R. Mattos, *Electrochim. Acta*., 41 (1996) 1165.
16. L.S. Kuburi, D.S. Yawas, S.Y. Aku and M.A. Adamu, *World J. Eng. Phys. Sci.,* 1 (2013) 26.
17. M. E. Olvera, J. Mendoza and J. Genesca, *J. of Loss Pre. in the Pro. Ind*., 35 (2015) 19.
18. NACE ID196, Laboratory Test Methods for Evaluating Oilfield Corrosion Inhibitors, *National Association of Corrosion Engineers,* (1996) Houston, TX, USA.
19. K. Magne, J. of Disp. *Sci. and Tech.,* 27 (2006) 587.
20. MA Migahed and IF Nassar, *Electrochim. Acta.,* 53 (2008) 2877.
21. MA Migahed, Ahmed A Farag, SM Elsaed and R Kamal, *Chemical Engineering Communications*., 199 (2012) 1335.
22. Q. B. Zhang and Y. X. Hua, *Electrochim. Acta.* 54 (2009) 1881.
23. Y. Chen, T. Hong, M. Gopal and W.P. Jepson, *Corrosion Science,* 42 (2000) 979.
24. B. Y. Fang, R. L. Eadie, W. X. Chen and M. Elboujdaini, *Corr. Eng. Sc. and Tech*, 45 (2010) 302.
25. Qiang Li, Haitao Hu and Y. Frank Cheng, *J. Pet. Sci. Eng.,* 147 (2016) 408.
26. J. Winiarski, W. Tylus and B. Szczygieł, *Appl. Surf. Sci.,* 364 (2016) 455.
27. Jinlong Lv and Hongyun Luo, *Journal of Nuclear Materials,* 452 (2014) 469.